Astron. Astrophys. 321, 207–212 (1997)

ASTRONOMY AND ASTROPHYSICS

The formation of black-holes in low-mass X-ray binaries

Simon F. Portegies Zwart[1], **Frank Verbunt**[1], **and Ene Ergma**[2]

[1] Astronomical Institute, Utrecht, Postbus 80000, 3508 TA Utrecht, The Netherlands
[2] Tartu University, Physics Department, Ülikooli 18, EE2400 Tartu, Estonia

Received 24 April 1996 / Accepted 12 September 1996

Abstract. We calculate the formation rates of low-mass X-ray binaries with a black hole. Both a semi-analytic and a more detailed model predict formation rates two orders of magnitude lower than derived from the observations. Solution of this conundrum requires either that stars with masses less than 20 $M_\odot$ can evolve into a black hole, or that stellar wind from a member of a binary is accompanied by a much larger loss of angular momentum than hitherto assumed.

Key words: binaries: close – stars: evolution – stars: neutron – X-rays: stars

1. Introduction

Six low-mass X-ray binaries currently are known to have a mass function that indicates a mass of the compact object larger than $\sim 3M_\odot$, and these are therefore believed to have a black hole accretor. All these systems are soft X-ray transients and the total number in the galaxy of such systems is estimated to be between a few hundred and a few thousand; at any moment in time only a small fraction is X-ray active (for reviews, see Cowley 1992, Tanaka & Lewin 1995, Tanaka & Shibazaki 1996).

The most popular formation scenario for low-mass X-ray binaries proposes a relatively wide binary with an extreme mass ratio as the progenitor system (van den Heuvel 1983). The massive star evolves to fill its Roche lobe and engulfs its low-mass companion. Due to the extreme mass ratio the low-mass star spirals into the envelope of the high-mass star. A close binary remains if the spiral-in ceases before the low-mass companion coalesces with the compact helium core of the primary. The helium core continues its evolution and may turn into a neutron star or a black hole. Only a few studies apply this evolutionary scenario specifically to the formation of low-mass X-ray binaries with an accreting black hole (see Romani 1992).

In this paper we discuss some problems of this standard formation scenario in its simplest form (Sect. 2) and show that these persist in a more refined treatment (Sect. 3). We quantify this in Sect. 4 and in Sect. 5 the results are discussed.

Send offprint requests to: Simon Portegies Zwart

2. Semi-analytic approach

In the standard scenario the formation of a low-mass X-ray binary starts with a high-mass primary and a low mass secondary star ($m_o \sim 1M_\odot$) in a detached binary. For simplicity we assume that the initial orbit is circular. As the primary evolves and expands to giant dimensions it fills its Roche lobe and starts to transfer mass onto its companion. Due to the small mass ratio mass transfer is highly unstable and results in a common-envelope phase. A close binary remains provided that the primary's envelope is fully ejected before the secondary star coalesces with the compact core of the primary. The reduction in the semi-major axis during the spiral-in can be computed by comparing the binding energy of the primary's envelope with the orbital binding-energy of the binary (Webbink 1984). The helium core continues its evolution and finally collapses into a neutron star or a black hole. The binary becomes an X-ray binary once the secondary star fills its Roche lobe.

We illustrate this scenario for primary stars of initially M_o = 20 and 60 $M_\odot$which reach a maximum radius of 1000 $R_\odot$(see Romani 1992). The scenario requires that the primary fills its Roche lobe during its evolution, i.e. that its Roche lobe has a radius less than 1000 $R_\odot$. The corresponding semi-major axis of the binary orbit may be calculated using the equation for the radius R_L of the Roche lobe given by Eggleton (1983):

$$\frac{R_L}{a} \equiv \mathscr{R}_L(q) = \frac{0.49}{0.6 + q^{2/3}\ln(1+q^{-1/3})}. \quad (1)$$

Here a is the semi-major axis of the binary and $q \equiv m/M$ is the mass ratio and R_L is the Roche-lobe radius for the star with mass M. For the 20 and 60 $M_\odot$primaries we thus find a semi-major axis of about 1590 and 1440 $R_\odot$, respectively.

The scenario further requires that the binary survives the spiral-in that follows upon the first Roche-lobe contact, i.e. that both the helium core and the 1 $M_\odot$companion star are smaller than their Roche lobes. The mass M_c and radius R_c of the helium

core of the primary can be computed with (see Iben & Tutukov 1985 and de Loore & Doom 1992, respectively)

$$M_{\rm c} = 0.073 M_o^{1.42}, \tag{2}$$

and

$$\log R_{\rm c} = -1.13 + 2.26 \log M_{\rm c} - 0.78 (\log M_{\rm c})^2. \tag{3}$$

The mass and radius of the secondary star are not affected by the spiral-in. The mass ratio after the spiral-in gives the sizes of the Roche lobes of the helium core and the secondary in units of the semi-major axis. From the radii of the helium star and its companion we can thus derive the minimum semi-major axis for which both stars fit inside their Roche lobes. For the 20 and 60 $M_\odot$primaries we thus find a semi-major axis after the spiral-in which should exceed 4.0 and 6.3 $R_\odot$, respectively. In both cases the most stringent limit is set by the main-sequence star.

The ratio of the semi-major axes before and after the spiral-in can be computed by comparing the binding energy of the primary's envelope with the binding energy released by the shrinking binary (see Webbink 1984):

$$\frac{a_f}{a_i} = \frac{M_{\rm c}}{M} \left(1 + \frac{2 a_i}{\alpha \lambda R} \frac{M_{\rm e}}{m} \right)^{-1}. \tag{4}$$

Here a_i and a_f are the semi-major axes at the onset and end of the spiral-in, and M and R are the mass and radius of the primary at the onset of spiral-in. We set $\alpha\lambda = 0.5$. We assume that the primary did not lose any mass before it fills its Roche lobe: $M = M_o$ and $M_{\rm e} = M_o - M_{\rm c}$. For the 20 and 60 $M_\odot$primaries we thus find a semi-major axis before the spiral-in which should exceed 1470 and 3160 $R_\odot$, respectively.

For the 20 $M_\odot$primary, the lower limit on the semi-major axis for survival of the spiral-in is smaller than the upper limit for Roche-lobe contact and a low-mass X-ray binary can be formed when the initial semi-major axis is between these two limits. For the 60 $M_\odot$primary, the lower limit on the semi-major axis for survival of the spiral-in is larger than the upper limit for Roche-lobe contact and no initial orbit leads to the formation of a low-mass X-ray binary: Roche-lobe overflow always leads to a merger.

Fig. 1 shows, as function of the mass of the primary, the lower and upper limits to the semi-major axis of the initial binary at which the binary survives the spiral-in and the primary reaches the Roche lobe. Only for low mass primaries ($M \lesssim 22 M_\odot$) does the binary survive the spiral-in. Thus, if only stars with an initial mass larger than 40 $M_\odot$(van den Heuvel & Habets 1984) form a black hole, the formation of a low-mass X-ray binary with a black hole as a compact object is excluded in the standard scenario.

One may argue that the binary survives the spiral-in even if the main-sequence star is larger than its Roche lobe after spiral-in, as long as the helium star fits inside its Roche lobe . The main-sequence star can shrink within its Roche lobe by transferring mass to the helium core. This mass transfer is stable because the main-sequence star is less massive than the helium core. In Fig. 1 we also show the lower limit to the semi-major axis obtained from the condition that only the helium star fits inside its Roche lobe. We see that even in this case low-mass X-ray binaries with a black hole cannot be formed in the standard scenario.

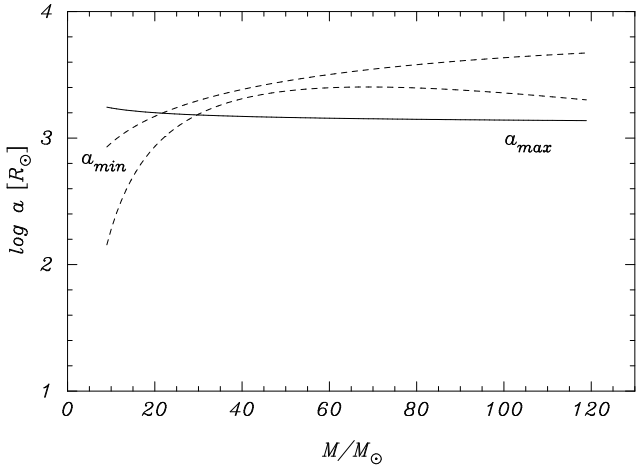

Fig. 1. Lower limit to the initial semi-major axis at which the binary survives the spiral-in, as function of the mass of the primary. The upper (lower) dashed line gives the limit determined from the condition that the secondary star (helium core) is smaller than its Roche-lobe, The solid line gives the upper limit at which the primary reaches its Roche lobe at its maximum radius of $R_{max} = 1000 R_\odot$. The secondary is assumed to be a 1 $M_\odot$star

3. Detailed model

Since the stellar parameters used in the previous Sect. are rather rough, the same computation is performed with a more detailed model for population I ($Z = 0.02$) stars. We use the models with moderate core overshooting computed by Schaller et al. (1992), using the radius (calculated from effective temperature and luminosity) and the mass of the star in the tabulated points. The mass of the star decreases as a function of time due to stellar wind. The mass loss in the stellar wind causes an increase of the Roche-lobe radius of the primary, (mainly) by increasing the semi-major axis and (to a lesser extent) by increasing the mass-ratio m/M. The increase in the semi-major axis is described, assuming an isotropic wind with high velocity according to the Jeans approximation, with (van den Heuvel 1983):

$$a(M + m) = \text{constant}. \tag{5}$$

The relation between the semi-major axis a_i at which the primary fills its Roche lobe R_L and the initial semi-major axis a_o is thus given by:

$$R_L = \mathscr{R}_L(q) a_i = \mathscr{R}_L \left(\frac{m}{M} \right) a_o \frac{M_o + m}{M + m}. \tag{6}$$

Here M_o and M are the zero-age mass of the primary and its mass at the moment it fills its Roche lobe. For each tabulated

point of the evolutionary track we equate the radius R of the primary to the Roche-lobe radius R_L in Eq. 6 to calculate the corresponding maximum initial semi-major axis a_o. The values for a_o and R for a 20 and a 60 $M_\odot$star accompanied by a 1 $M_\odot$companion are shown in Fig. 2. A value for a_o smaller than reached at an earlier stage of the evolution implies that Roche lobe overflow would have occurred at that earlier moment.

For each tabulated point of the evolutionary track we calculate the mass of the envelope M_e by subtracting the core mass from the total mass. Because the stellar evolution models incorporate overshooting, which tends to increase the core mass, we calculate the core mass by multiplying the value found from Eq. 2 with 1.125 (Maeder & Meynet 1989). We also know the minimum separation after spiral-in for a detached binary. From this we calculate the minimum separation at the onset of spiral-in with Eq. 4, and the minimum separation of the initial binary $a_{o,m}$ with Eq. 6. These minimum separations are also shown in Fig. 2.

The value of a_o of the first evolutionary point at which $a_o > a_{o,m}$, which we denote as a_{min}, corresponds to the minimum initial separation that the binary must have to survive the spiral-in. The maximum of the values of a_o for all evolutionary stages, indicated with $a_{o,max}$, corresponds to the maximum initial separation of the binary at which the primary can reach its Roche lobe. Only binaries with an initial separation in the range a_{min} – $a_{o,max}$ can evolve into low-mass X-ray binaries. For a 20 $M_\odot$primary with a 1 $M_\odot$secondary this range is 1000 – 1590 $R_\odot$.

The Roche lobe can only be reached for the first time in those evolutionary stages for which a_o is larger than the a_o's at all earlier evolutionary stages. Those stages are marked in Fig. 2 with •. Note that core hydrogen burning ends in tabulated point 13, and helium core burning begins in point 21. Helium core burning ends in point 43, and carbon burning starts in point 46. For a star of $\sim 5M_\odot$, the radius of the star expands following the end of core hydrogen burning, and mass transfer during this first ascent of the giant branch is called case B. At the onset of core helium burning, the star shrinks. It expands once more after the end of core helium burning, and mass transfer during this second ascent of the giant branch is called case C. For the $20M_\odot$ star shown in Fig. 2, however, the radius does not shrink at the onset of each new phase of core fusion, but continues its expansion throughout its evolution, once the Hertzsprung gap is passed. The $60M_\odot$ shrinks at the onset of helium fusion in the core, mainly due to extensive mass loss.

As shown by Fig. 2 a 60 $M_\odot$ primary with a 1 $M_\odot$ secondary can, according to the same reasoning, only evolve into a low-mass X-ray binary if its semi-major axis is in the very small range of 980 – 1100 $R_\odot$.

We determine the mass and size of primaries in a range of masses at the moment they fill their Roche lobes at $a_{o,max}$ for each tabulated stellar evolution track. The masses and radii at $a_{o,max}$ of the stars that are not tabulated by Schaller et al. (1992) are determined by a linear interpolation between the tabulated

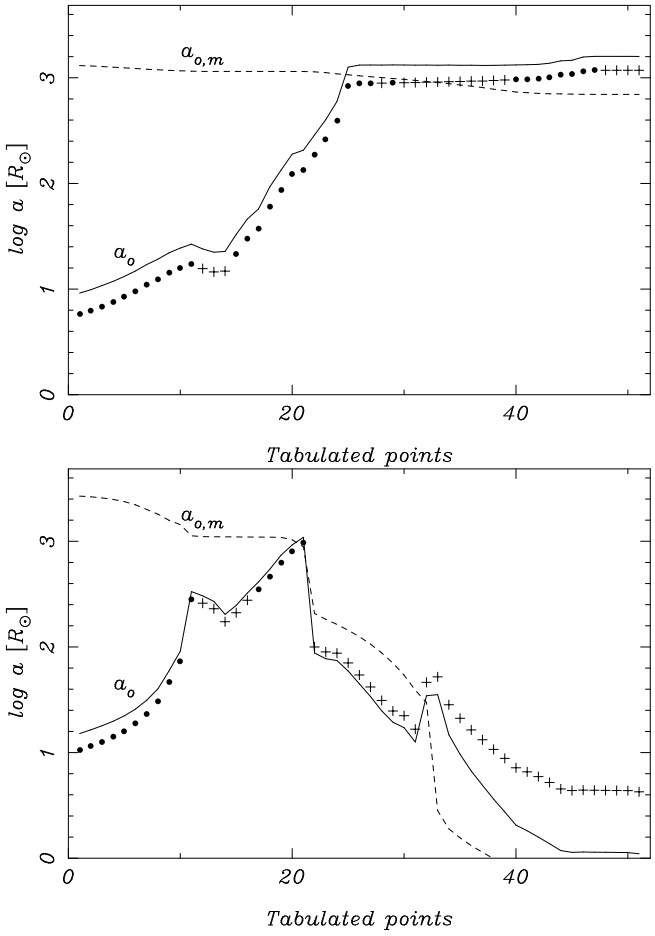

Fig. 2. a • and + indicate radii for subsequent evolutionary stages of the 20 $M_\odot$ primary as tabulated in Schaller et al. (1992). From the mass of the primary at the tabulated point one may calculate the semi-major axis of a binary with a 1 $M_\odot$ secondary in which the primary fills its Roche lobe, and from this the semi-major axis a_o, shown as a solid line, of the binary at the beginning of its evolution. For each tabulated evolutionary stage we calculate the minimum semi-major axis at which the core of the primary survives the spiral-in of a 1 $M_\odot$ companion, and from this the minimum semi-major axis $a_{o,m}$, indicated with the dashed line, of the binary at the beginning of its evolution. Primaries at the evolutionary stages marked with a + cannot fill their Roche lobe for the first time at that stage but will reach their Roche lobe at an earlier point in their evolution. A low mass X-ray binary is formed when $a_o > a_{o,m}$ for evolutionary stages indicated with •. **b** as **a** for a 60 $M_\odot$primary

models. The resulting values for $a_{o,max}$ are shown as a solid line in Fig. 3.

If Roche-lobe overflow for all initial semi-major axes smaller than $a_{o,max}$ leads to a merger, then a_{min} is not properly defined. A lower limit can be obtained by computing a_{min} with the stellar parameters that correspond to the point where $a_{o,max}$ is reached.

Mass loss from stars more massive than $\sim 100M_\odot$ is so copious that these stars lose their entire hydrogen envelope before they expand on the giant branch, i.e. before Roche-lobe

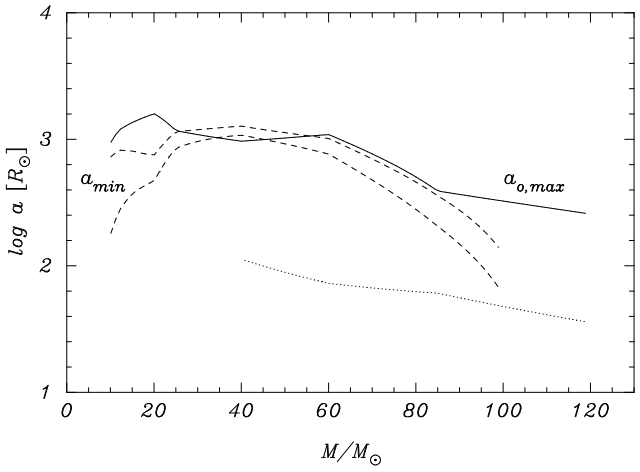

Fig. 3. Lower limit to the initial semi-major axis at which the binary survives the spiral-in, as function of the initial mass of the primary, calculated with use of the evolutionary sequences by Schaller et al. (1992). The upper (lower) dashed line gives the limit determined from the condition that the secondary star (helium core) is smaller than its Roche-lobe, The solid line gives the upper limit at which the primary reaches its Roche lobe at its maximum radius of $R_{max} = 1000 R_\odot$. The secondary is assumed to be a 1 $M_\odot$star. The dotted line indicates the initial semi-major axis of a binary in which a 1 $M_\odot$ secondary can fill its Roche lobe after the primary has lost its entire envelope without ever having filled its Roche lobe

contact is achieved. The common-envelope phase hardly leads to a spiral-in, whereas further attrition of the core to a small final mass ($\sim$ 8 $M_\odot$ according to Schaller et al. 1992) causes the binary orbit to expand. As a result the final orbit is so wide that the 1 $M_\odot$ secondary never reaches its Roche lobe.

Fig. 3 shows, as a function of the zero-age mass of the primary, the lower limits to the semi-major axis of the initial binary at which the binary survives the spiral-in a_{min} (or its conservative lower limit), and the upper limit for which the primary reaches its Roche lobe $a_{o,max}$.

Comparison of Fig. 3 with Fig. 1 illustrates that the mass loss of massive stars and the concurrent widening of the binary reduces the maximum initial separation for which the binary reaches Roche-lobe contact. For stars with $\sim$ 70 $M_\odot$ the maximum stellar radius is smaller than 1000 $R_\odot$, which leads to a further reduction of $a_{o,max}$. The wind mass-loss affects the minimum initial separation necessary to survive the spiral-in in two ways: the widening of the orbit reduces this separation, whereas the reduction of the envelope mass enlarges it.

Fig. 3 indicates that the formation rate of low-mass X-ray binaries with a neutron star greatly exceeds the formation-rate of low-mass X-ray binaries with a black hole, because the range of allowed initial separations is larger for neutron star progenitors.

Romani (1992) mentions the possibility that the secondary star might fill its Roche lobe as it evolves on the asymptotic giant-branch after the primary collapsed into a remnant without ever having reached Roche-lobe contact. If this happens the binary orbit also widens dramatically, according to Eq. 5. If the orbit widens too much, the secondary will not reach its Roche lobe. In Fig. 3 we show the maximum initial semi-major axis for which a 1 $M_\odot$ star can reach its Roche lobe after its companion has lost its envelope. It is seen that this semi-major axis is so small, that it invalidates the assumption that Roche lobe contact of the primary has been avoided.

4. Galactic formation rates

The formation rate of binaries that reach Roche-lobe contact and survive the spiral-in can be estimated by computing the birth rate of binaries with suitable initial parameters; primary mass, mass ratio and semi-major axis. For simplicity we neglect the eccentricity. For the initial mass function for the primary we use a Salpeter function (Salpeter 1964) integrated over the Galaxy:

$$\Psi_G(M) = 0.05 M^{-2.35} \, [M_\odot \ \mathrm{yr}^{-1}]. \qquad (7)$$

This normalization gives a supernova rate in agreement with the observed rate. The initial semi-major axis distribution $\Gamma(a)$ is taken flat in $\log a$ (Kraicheva et al. 1978). We assume a flat initial mass-ratio distribution, $\Phi(q) = 1$. For a given mass of the primary M the fraction of binaries with a mass of the secondary between $(m - \epsilon)$ and $(m + \epsilon)$ is then proportional to $2\epsilon/M$.

Primaries with an initial mass between 10 and 40 $M_\odot$ are assumed to leave a neutron star after the supernova, progenitors with a mass between 40 and 100 $M_\odot$ form black holes. The mass of the secondary is taken to be 1 $M_\odot$. The minima and maxima for the initial semi-major axis are computed as described in the previous section. We integrate the initial distribution functions for the primary mass, the mass ratio and the semi-major axis between the mass limits M_{min} and M_{max} and the corresponding limits for the semi-major axis a_{min} and $a_{o,max}$ (see Fig. 3):

$$Br = \int_{M_{min}}^{M_{max}} \int_{a_{min}}^{a_{o,max}} \Psi_G(M) \frac{2\epsilon}{M} \Gamma(a) \, da dM \, [\mathrm{yr}^{-1}]. \qquad (8)$$

With $\epsilon = 0.15$ $M_\odot$, with a binary fraction of 50% of high mass stars, and with the lower limit to a_{min} set by the main-sequence star, the galactic formation rate of binaries that reach Roche-lobe contact and survive the spiral-in is $2.2 \cdot 10^{-6}$ yr^{-1} for the binaries with a neutron star and $9.6 \cdot 10^{-9}$ yr^{-1} for the black-hole binaries. The formation rate thus calculated for the low-mass X-ray binaries with a neutron star is compatible (within the rather wide uncertainties) with the rate derived from the observed numbers of such binaries. The formation rate of low-mass X-ray binaries with a black hole is about 1% of the formation rate of low-mass X-ray binaries with a neutron star, whereas the observations indicate equal formation rates for these two types of binaries.

5. Discussion

We briefly discuss the assumptions and model uncertainties that affect our computations most.

In our calculations the effect of convective overshooting on the mass of the helium core is taken into account in a relatively simple manner, since the tabulated stellar evolution tracks do

not provide masses for the stellar helium core. The importance of convective overshooting is uncertain, and therefore we investigate small variations in its effects.

If we increase the mass of the core by increasing the multiplication factor for Eq. 2 discussed in paragraph 2 of Sect. 3 from 1.125 to 1.250, the lower limit a_{min} to the semi-major axis for which a binary survives the spiral-in is slightly reduced, and consequently the birthrate of neutron star binaries is enhanced by $\sim$ 28%, and the birthrate of black hole binaries increases with a factor $\lesssim 4$. An increase of the exponent in Eq. 2 to 1.57, which is not unrealistic according to Iben & Tutukov (1985), reduces the discrepancy between the birthrates for black holes and neutron stars in low-mass X-ray binaries to a factor 15. Thus neither of these changes in Eq. 2 leads to a sufficiently high birthrate of black-hole binaries relative to neutron-star binaries.

The efficiency $\alpha\lambda$ at which the common-envelope is expelled upon the spiral-in is highly uncertain. The effect of varying $\alpha\lambda$ on the galactic formation rate for binaries that reach Roche-lobe contact and survive the spiral-in is demonstrated in Fig. 4. Decreasing $\alpha\lambda$ results, as expected, in a strong reduction in the formation rate of low-mass X-ray binaries with a neutron star as well as with a black hole. By increasing $\alpha\lambda$ to a value larger than about unity, the formation rate of low-mass X-ray binaries approaches a constant rate, limited by the number of primordial binaries formed in the galaxy. Note that $\alpha\lambda$ might have different values for neutron star– and black-hole progenitors.

To investigate the effect of the stellar metallicity on the formation rate of low-mass X-ray binaries we compute two more models using the evolutionary tracks calculated by Charbonnel et al. (1993) for Z = 0.004 and Schaerer et al. (1993) for Z = 0.04 (see Fig. 4). Apart from the enhanced mass-loss rates in the model with high metallicity which results in a larger formation rate of low-mass X-ray binaries, these model variations have little influence on our conclusions. The models with a lower metallicity lose less mass in the stellar wind and the fraction of binaries that survive the spiral-in decreases accordingly.

The limit of $\sim 40 M_\odot$, which we use throughout the calculations, was originally derived from the observation of the high-mass X-ray binary LMC X-3 (van den Heuvel & Habets 1984). Recently the analysis of the data of Wray 977, the BIa hypergiant companion of the X-ray pulsar GX301-2, has increased the empirical lower mass limit for the formation of a black-hole in a binary to $M_o \sim 50\ M_\odot$ (Kaper et al. 1995). This only exacerbates the problem of too low a formation rate of black-hole binaries in our calculations. Maeder (1992) argues on the basis of the galactic ratio of the abundances of metals and of helium that the lower limit for the formation of a black hole is 20 – 25 $M_\odot$. As can be seen in Fig. 3, such decrease of the lower mass-limit has little effect on our computations, because $a_{min} > a_{o,max}$ in the range of 25–40 $M_\odot$.

The stellar evolutionary tracks of Schaller et al. (1992) follow the single stars beyond the point of carbon burning. The large amount of mass and angular-momentum lost in the stellar wind during earlier phases of the evolution of the more massive primaries cause the binary orbit to widen and prohibits mass transfer after the onset of core helium burning (see Fig. 2). For the amount of angular momentum lost per unit mass in the stellar wind we used the standard description of isotropic mass loss from the donor (see Eq. 5). Mass transfer at an evolutionary stage well after the onset of helium fusion (say, beyond point 25 in Fig. 2) can only be an effective channel for the formation of low-mass X-ray binaries with a neutron star as the compact object, if the loss of angular momentum is high enough for the orbit to shrink. For a more massive progenitor, larger than $\sim 40 M_\odot$, which leaves a black hole instead of a neutron star after the supernova, such late mass transfer is not likely to become important even for such high loss of angular momentum: the star has evolved into a naked helium core and a merger will be unavoidable upon Roche-lobe contact.

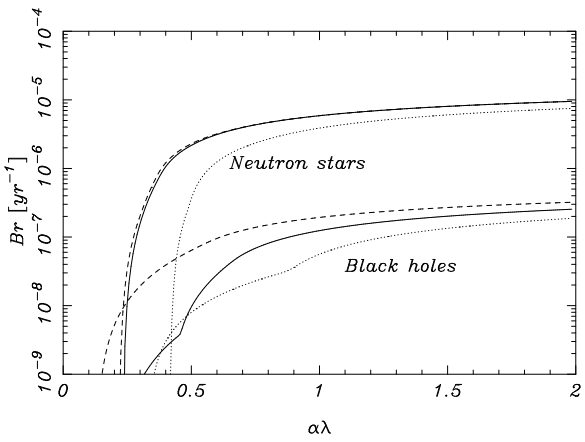

Fig. 4. Birthrate (per year in the galaxy) of low-mass X-ray binaries with a neutron star (upper lines) and a black hole companion (lower lines) as function of the common-envelope efficiency-parameter $\alpha\lambda$. The full lines are from the stellar evolution models from Schaller et al. (1992), the dotted lines are from the low metallicity models with Z = 0.004 from Charbonnel et al. (1993) and the dashed lines are computed with Z = 0.040 from Schaerer et al. (1993)

The evolution of the helium star and the effect of the supernova on the binary orbit are neglected in our calculations: both effects tend to lower the formation rate of low-mass X-ray binaries (see e.g. Portegies Zwart & Verbunt 1996). Mass transfer from the helium star to its companion can result in a merger and the asymmetry of a supernova can dissociate the binary. Both effects, however, tend to reduce the formation-rate of neutron stars as well as black holes in low-mass X-ray binaries and do consequently not solve the birth-rate problem discussed in this paper.

6. Conclusions

Our computations, in contradiction to the results of Romani (1992), predict a formation rate for low mass X-ray binaries with a black hole which is much smaller than the value derived from the observed numbers and estimated X-ray lifetime. The striking difference between our and his results can be seen immediately by comparing his Fig. 1 with our Fig. 1. Romani's

values for a_{max} are much higher than ours: this is due to the fact that he uses $1/q$ instead of q in the equation for the Roche lobe (our Eq. 1). (This error has been silently corrected in Romani 1994.) This is true both for binaries in which mass transfer preceeds the supernova explosion, and for binaries in which the primary explodes after losing its envelope without ever having filled its Roche-lobe. The discrepancy between theoretical and observed formation rates cannot be solved by invoking different metallicities for the progenitor systems, nor by assuming different efficiencies for the envelope ejection during spiral-in.

Black-hole binaries can be produced in larger numbers only if it is assumed that stars with initial masses less than approximately 20 $M_\odot$ can collapse to black holes; or alternatively if it is assumed that the angular momentum loss caused by the stellar wind is so high that the binary orbit shrinks; or alternatively if the collapse of a helium core to a black hole is asymmetric, so that the post-supernova orbit can be smaller than the pre-supernova orbit (see Portegies Zwart & Verbunt 1996).

Acknowledgements. This work was supported in part by the Netherlands Organization for Scientific Research (NWO) under grant PGS 78-277.

References

Charbonnel, C., Meynet, G., Maeder, A. S., Schaller, G., Schaerer, D. 1993, A&AS, 101, 415
Cowley, A. 1992, ARA&A, 30, 287
de Loore, C. W. H., Doom, C. 1992, Structure and evolution of single stars and binaries, Kluwer Academic Publishers, Dordrecht, 179
Eggleton, P. 1983, ApJ, 268, 368
Iben, I. J., Tutukov, A. V. 1985, ApJS, 58, 661
Kaper, L., Lamers, H., Ruijmakers, E., van den Heuvel, E., Zuiderwijk, E. 1995, A&A, 300, 446
Kraicheva, Z. T., Popova, E. I., Tutukov, A. V., Yungelson, L. R. 1978, AZh., 55, 1176
Maeder, A. 1992, A&A, 264, 105
Maeder, A., Meynet, G. 1989, A&A, 210, 155
Portegies Zwart, S. F., Verbunt, F. 1996, A&A, 309, 179
Romani, R. W. 1992, ApJ, 399, 621
Romani, R. W. 1994, in A. W. Shafter (ed.), Interacting Binary Stars, ASP Conf. Ser. 56, p. 196
Salpeter, E. E. 1964, ApJ, 140, 796
Schaerer, D., Charbonnel, C., Meynet, G., Maeder, A. S., Schaller, G. 1993, A&AS, 102, 339
Schaller, G., Schaerer, D., Meynet, G., Maeder, A. S. 1992, A&AS, 96, 269
Tanaka, Y., Lewin, W. H. G. 1995, in W. H. G. e. a. Lewin (ed.), X-ray binaries, Cambridge University Press, 536
Tanaka, Y., Shibazaki, N. 1996, ARA&A, 34, 607
van den Heuvel, E. 1983, in W. Lewin, E. van den Heuvel (eds.), Accretion-driven stellar X-ray sources, Cambridge U.P., Cambridge, p. 303
van den Heuvel, E., Habets, G. 1984, Nat, 309, 598
Webbink, R. F. 1984, ApJ, 277, 355

This article was processed by the author using Springer-Verlag LaTeX A&A style file *L-AA* version 3.